PHYSICAL REVIEW B VOLUME 26, NUMBER 12 15 DECEMBER 1982

Time-resolved optical studies of silicon during nanosecond pulsed-laser irradiation

Douglas H. Lowndes, G. E. Jellison, Jr., and R. F. Wood
Solid State Division, Oak Ridge National Laboratory, Oak Ridge, Tennessee 37830
(Received 19 July 1982)

The time-resolved optical transmission (at 1152-nm wavelength) and reflectivity (at both 633 and 1152 nm) of crystalline silicon have been measured with ~nsec resolution during and immediately after pulsed-ruby-laser irradiation (694 nm, full width at half maximum pulse duration 14 nsec), over a range of pulsed-laser energy densities E_l. For $E_l \geq 0.8$ J/cm^2 the transmission is found to go to zero and to remain at zero for a time proportional to E_l (during which time the reflectivity is also at a maximum value), and then to recover (in ~500 nsec) to its initial value. The zero-transmission result during the high-reflectivity phase contradicts reports of other similar experiments. Measured reflectivities during the high-reflectivity phase agree with reflectivities calculated from the known optical constants of molten silicon, at both the 633- and 1152-nm probe wavelengths. Intense near-band-gap photoluminescence is also observed from our silicon samples, for E_l both above and below the threshold for the high-reflectivity phase. The results of detailed calculations using the thermal-melting model are presented. Good quantitative agreement is found between the results of these calculations and the measured melting threshold of 0.8 J/cm^2, and with the reflectivity and transmission of crystalline silicon, as functions of time and E_l. The small ($\lesssim 10\%$) absorption due to long-lived laser-induced free carriers is also calculated and found to be in satisfactory agreement with the measured transmission for long ($\gtrsim 100$ nsec) times after pulsed-laser irradiation. The results are discussed in relation to other recent time-resolved measurements during pulsed-laser irradiation of silicon.

I. INTRODUCTION

During the past several years, pulsed lasers have been used to remove lattice damage, to recrystallize amorphous near-surface regions, and to electrically activate implanted dopant ions in ion-implanted samples of both elemental and compound semiconductors.[1–4] The experiments used to assess the results of pulsed-laser irradiation and to test theoretical understanding of the physical phenomena involved fall into two categories: (1) conventional post-annealing measurements such as Rutherford backscattering, secondary-ion mass spectroscopy, transmission electron microscopy, and scanning electron microscopy, and (2) time-resolved measurements, such as time-resolved optical reflectivity and transmission, using visible and near-ir probe beams,[5–10] as well as time-resolved measurements of electrical conductivity,[11] time-resolved Raman temperature measurements,[12,13] and time-resolved x-ray diffraction.[14]

Time-resolved measurements of physical properties during and immediately after pulsed-laser irradiation are useful in revealing changes in the time scale for annealing and recrystallization as a function of changes in the initial state of amorphization and/or chemical composition of the near-surface region. They also provide a stringent test of theoretical models for the laser-annealing process, which incorporate a number of optical and thermal parameters of the target material. Time-resolved measurements allow the model calculations to be calibrated and "fine tuned" to the effect of systematic changes in any one parameter (e.g., the near-surface optical-absorption coefficient). Time-resolved measurements are also capable, in principle, of determining the time scale for energy transfer from the excited electron-hole pairs, created by absorption of pulsed-laser radiation, to the lattice. However, measurements with nsec resolution only indirectly address this question, because, at the high carrier densities ($\lesssim 10^{21}$ cm^{-3}) produced by pulsed lasers, carrier-phonon relaxation occurs very rapidly[15] ($\lesssim 10^{-12}$ sec). The rapid energy transfer to the lattice is greatly enhanced by Auger recombination and subsequent thermalization of hot Auger carriers by way of phonon emission.[16]

Because of their sensitivity to processes occurring

during and immediately after laser irradiation, time-resolved measurements have recently become the focal point of a theoretical controversy regarding the physical mechanism for pulsed-laser annealing, in connection with "thermal" versus "nonthermal" models for the annealing process. The thermal-melting model[17,18] of pulsed-laser annealing (PLA) assumes that the laser energy absorbed by the sample is transferred to the lattice in a time less than the laser-pulse duration ($\sim$10 nsec) and that thereafter normal heat transfer and melting occur. This model is now supported by an impressive array of experimental and theoretical results.[5,6,9,10,17–22]

Recently, however, Compaan and co-workers published results of a series of experiments which they claim provide proof that the thermal-melting model for PLA cannot be correct.[7,8,12,13,23] In two separate series of time-resolved experiments, using slightly different wavelengths and pulse durations for excitation and probe-laser pulses, these authors used the ratio of Stokes to anti-Stokes Raman intensities to measure the lattice temperature of crystalline silicon (*c*-Si) shortly after the end of the high-reflectivity phase (HRP) induced by pulsed-laser irradiation.[12,13,23] They concluded that the lattice temperature is so low [$\sim$300 °C (Ref. 12) or $\sim$400 °C (Ref. 23), within 10 or 30 nsec after the end of the HRP, respectively] that "this enhanced reflectivity phase cannot be the usual 1400 °C molten phase of silicon unless unrealistically large cooling rates are assumed."[23]

Compaan and co-workers have also carried out a series of time-resolved transmission and reflectivity measurements using both *c*-Si and silicon-on-sapphire (SOS) samples.[7,8,23] Their initial transmission measurements[7] at $\lambda = 1.15$ μm were reported to show large, finite transmission through a $\sim$0.4-mm thick *c*-Si sample during the HRP. Following our initial reports[9,10] of the experiments described in detail in this paper, it was established that the transmission reported in Refs. 7, 8, and 23 was an experimental artifact resulting from use of a Ge *p-i-n* diode with a spatially varying detector response time.[23] However, further time-resolved optical experiments by Compaan and co-workers using both *c*-Si and SOS have led them to conclude that a laser pulse with E_I sufficient to produce the HRP induces only a very thin ($\sim$70-nm thick), highly absorbing layer at the sample surface, within which the absorption coefficient is $\sim 7\times 10^5$ cm^{-1}. They conclude[23] that either (1) the HRP is not the normal 1400 °C phase of molten silicon, but possibly the cooler high-density "plasma annealing" phase suggested by Van Vechten *et al.*,[24] or (2) there is a large amount of undercooling present in the fluid (molten) silicon at the recrystallizing fluid-solid interface.

The time-resolved transmission and reflectivity measurements summarized here were undertaken to provide an experimental check on the results initially reported by Compaan *et al.*, as well as to provide more extensive data for detailed testing of thermal-melting model calculations. Our experiments also required testing a number of diode detectors with $\sim$nsec response time and resulted in the discovery of one detector capable of faithfully following both rising and falling transient light signals (a problem which has now been investigated in more detail elsewhere[25]). The model calculations reported below, together with new measurements of the high-temperature optical properties of *c*-Si,[26] provide the first detailed test of the ability of thermal-melting model calculations to simultaneously describe both transmission and reflectivity measurements, with *no* free parameters. As is shown below, the measurements and calculations are in good agreement with each other, as well as with known optical properties of molten silicon.

II. EXPERIMENTAL

Experiments were carried out using a pulsed ruby laser ($\lambda = 694$ nm) operated in the TEM_{00} mode with 14 ± 1 nsec [full width at half maximum (FWHM)] pulse duration. The samples were polished, $\sim$400-μm thick, *c*-Si wafers (phosphorus-doped, 2–7 Ω cm); for transmission measurements the samples were polished on both sides to eliminate scattering of the 1152-nm probe laser beam. The samples were located 9.8 m beyond the second amplifier stage of the pulsed ruby laser and 75 cm beyond an $f_L = 1.0$ m converging lens; this arrangement resulted in only a slow variation of energy density over the 4-mm-diam central part of the laser beam. However, the irradiated sample area was limited to a 2- or 3-mm-diam region by a thin mask placed directly over the sample. Calorimetric measurements of E_I in the region sampled by the probe laser beam were carried out through a carefully centered 1-mm-diam aperture.

Measurements were carried out using a wide range of experimental conditions. Initial transmission measurements were made with an unfocused 2-mW cw He-Ne probe laser beam ($\lambda = 1152$ nm,

$1/e^2$ diam=0.97 mm) incident at 14° to the sample normal, and detected without the use of collection optics. An extensive series of experiments were carried out later with this beam incident at 4.7°, focused to a ~230-μm, $1/e^2$-diam spot on the sample, and refocused onto the detector with various image-object distances and collection optics. Our observation of a period of zero transmission was found to be entirely independent of probe beam focusing and/or the use of collection optics. Thus, the results we obtained are not experimental artifacts resulting from scattering, deflection, and/or self-defocusing of the probe beam off the detector due, for example, to a change in index of refraction during the HRP.[27]

A Si avalanche photodiode (APD; active region 1.5-mm diam, 2-nsec rise and fall times), a Ge *p-i-n* photodiode, a Ge APD, and an InAs photodiode were all tested for use in the transmission experiments. The latter two detectors were quickly eliminated because of low sensitivity at the low bias voltage necessary (InAs) and changes in detector response time with bias voltage (Ge APD). The Ge *p-i-n* diode was also eliminated because its responsivity is a factor of 10 less than that of the Si APD at 1152 nm, and because it exhibited both zero baseline overshoot (on a falling light signal) and a long recovery time (~600 nsec time constant). Similar detector response problems, on falling light signals, have now also been investigated by others.[23,25] A 1152-nm bandpass filter (10-nm bandwidth and ~40% transmission) was necessary directly in front of the Si APD detector, in order to prevent intense near-band-gap photoluminescence emitted by the sample from swamping the detector when it was close (~9 mm) to the sample.

A 3.4-mW cw HeNe laser (λ=633 nm), unfocused and incident at 12° to the sample normal, or focused to 140 μm ($1/e^2$ diam) and incident at 4.7°, and the Si APD were used for the reflectivity measurements. The APD's high red sensitivity made it necessary to use three 633-nm 1% bandwidth (FWHM) filters in front of it, to block the ruby-light pulse. The 1152-nm probe laser was also used for reflectivity measurements, as described above.

Three separate storage oscilloscope recordings (on successive ruby-laser shots) with (a) both probe beam and ruby beam present, (b) probe beam blocked, and (c) both beams blocked, allowed a clean separation of the transmission or reflectivity signal from near-band-gap photoluminescence and radiated electromagnetic noise (associated with firing the pulsed laser). The measured quantities are ratios of transmission or reflectivity during the HRP to the initial transmission (T_0) or reflectivity (R_0); these ratios were converted to absolute transmission or reflectivity values using separate measurements of T_0 and R_0. For our *c*-Si, the measured T_0=0.518 at 1152 nm and 4.7° is in excellent agreement with the value T_0=0.514 calculated from room-temperature optical constants for Si (Refs. 28 and 29) (including multiple internal reflections and a 2% absorption loss). The specular component of R_0 was 0.391 (using the same unfocused beam geometry as in the time-resolved measurements), somewhat smaller than the calculated value of 0.465. Thus, about 7% of the reflected light at 1152 nm is diffuse. At 633 nm the measured and calculated R_0 equaled 0.347.

III. RESULTS AND DISCUSSION

A. Transmission

Figure 1 shows typical results of a series of transmission measurements, with E_l both below and above the threshold (E_l~0.8 J/cm^2) for the HRP. The transmission of the focused 1152-nm probe beam drops to zero, and remains at zero, for a period of time τ_m that increases with increasing E_l. A background signal, primarily near-band-gap photoluminescence transmitted through the 1% bandpass filter, was subtracted from the measured signal (using successive laser shots, as described above) to obtain the data of Fig. 1.

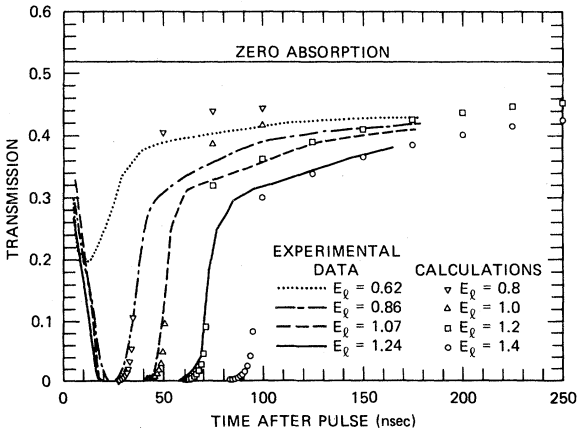

FIG. 1. Time-dependent transmission of the 1152-nm focused probe-laser beam through *c*-Si during and after pulsed ruby-laser irradiation. Lines: experimental data. Discrete points: model calculations (see text). T_0=0.518 is also shown.

The subtraction procedure for eliminating the background signal was found to give highly reproducible results on successive laser shots, as illustrated by Fig. 2. The presence of weak near-band-gap photoluminescence during part of the zero transmission period verifies that the detector is responding during this time. The linearity of the detector was also checked over a wide dynamic range. The minimum transmission observed was indistinguishable from zero, while the maximum that could be present and remain undetected was estimated to be less than 1%. We note that our result of zero transmission during the HRP contradicts the results reported by Lee *et al.*[7]

Figure 1 also shows results of calculations of the time-dependent transmission through *c*-Si at several E_l values. The melting-model calculations were carried out using the macroscopic diffusion equation, cast into finite difference form for numerical solution on a closely spaced mesh of points in space and time, to describe the heat flow. The basic computer program and procedures used have been described elsewhere in detail.[17,19] However, it was necessary to revise the program in order to include the temperature-dependent optical properties. A description of the revisions and illustrations of the importance of the temperature-dependent optical properties in melting-model calculations is given by Wood *et al.*[30] The values used for the various thermal and optical parameters in the present calculations are shown in Table I. The temperature dependence of the optical-absorption coefficient was taken from the recent work of Jellison and Modine[29] while that of the reflectivity (at $\lambda = 693$ nm) for *c*-Si was estimated from the literature. The primary theoretical results of these melting-model calculations are plots of (a) melt depth versus time (Fig. 3) and (b) time-dependent profiles of temperature vs depth in the solid below the molten layer and after the molten layer has recrystallized (Fig. 4). These were used as input data for the calculations of transmission as a function of time. Published values for the optical constants for molten Si (Ref. 26) were used to calculate the attenuation due to the molten layer, while new measurements[31] of the optical properties of *c*-Si at 1152 nm as a function of temperature were used for the hot *c*-Si. Thus *no* free parameters are involved in the time-dependent transmission calculations. The optical properties measurements[26,31] show that when the melt front is many skin depths from the silicon surface, virtually no light can penetrate the molten Si. As the melt front reaches ~4 skin depths, some of the 1152-nm radiation is able to penetrate the molten region, as well as the rest of the sample; as the recrystallization front approaches the sample surface, more and more light is able to penetrate the molten layer, and hence to be detected. This transmission has been calculated, and is shown in Fig. 1 by the calculated points near zero transmission. When the melt front has reached the surface, the recrystallized near-surface region is still hot (see Fig. 4), and the absorption coefficient is still substantially above the room-temperature value (see Ref. 31); this leads to enhanced absorption, with the calculated transmission shown in Fig. 1 by the points approaching the zero transmission line. As Fig. 1 shows, both the detailed shape of the calculated return to finite transmission (following the zero-transmission period) and the E_l dependence of the transmission are in good agreement with the experimental results.

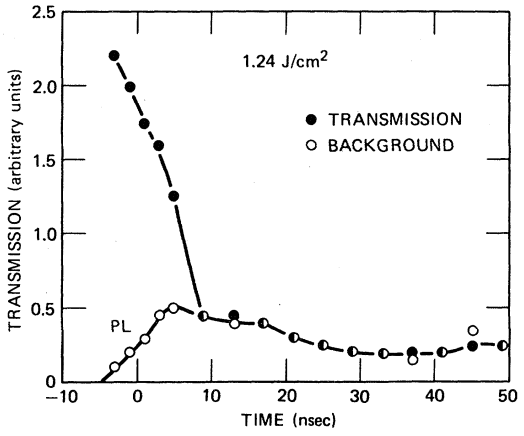

FIG. 2. Time-dependent T signals on successive pulsed ruby-laser shots (●) with and (○) without the 1152-nm probe-laser beam, illustrating the reproducibility of the procedure for subtracting residual near-band gap photoluminescence and radiated electromagnetic noise from the T signal.

Careful comparison of the experimental and calculated results in Fig. 1, for times well after the zero-transmission period, reveals that the experimental transmission is $\lesssim 0.05$ lower than that calculated. This suggests the presence of $\lesssim 10\%$ additional free-carrier absorption (not included in the melting calculations).

In order to estimate the magnitude of free-carrier absorption that is likely to be present, due to carriers remaining in the near-surface region for times $\gtrsim 100$ nsec, we make use of the fact that any initial high (laser melting induced) carrier concentration will be rapidly reduced by Auger recombination. The known Auger recombination rate for electrons

TABLE I. Input data for crystalline silicon melting model calculations.

Quantity	Value used and comments
Thermal conductivity	Temperature dependent; see text and Fig. 1 of Ref. 17
Specific heat	As above
Density	2.3 g/cm^3 ($\sim$10% change on melting ignored)
Reflectivity	
solid (694 nm)	$0.34 + 0.000\,054T$ (°C)
liquid	0.70 (see text)
Absorption coefficient (694 nm)	$2540\exp(T/427\,°\text{C})$ (see text)
Latent heat of melting	430 cal/g
Melting temperatures	1410°C
Substrate temperature	20°C
Laser pulse	Triangular; see Ref. 17
duration	15 nsec (FWHM)
energy density	Varied

(holes) in silicon,[32] $\tau_n^{-1}=C_n n^2$ ($\tau_p^{-1}=C_p p^2$) with $C_n=2.8\times10^{-31}$ ($C_p=1\times10^{-31}$) cm^{6}sec^{-1}, can be used to estimate a self-consistent average carrier density at $t=100$ nsec. (We use rate constants measured for a nondegenerate carrier system, since these are the only values currently available.) Thus $\tau_A^{-1}\simeq\tau_n^{-1}+\tau_p^{-1}$ with $\tau_A\geq100$ nsec requires $n=p\lesssim5\times10^{18}$ cm^{-3}. [C_n and C_p are nearly independent of temperature over the (0—400)-K range.[32]] Taking the diffusion coefficient for carriers to be $D\sim3.5$ cm^{2}sec^{-1} (mobility ~45 cm^2/volt sec) at high carrier densities,[33] we find that

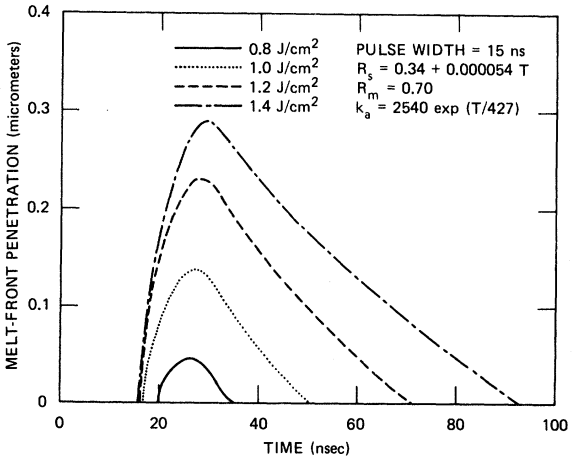

FIG. 3. Profiles of melt front penetration vs time for c-Si, generated using the thermal-melting model with the parameter values given in Table I.

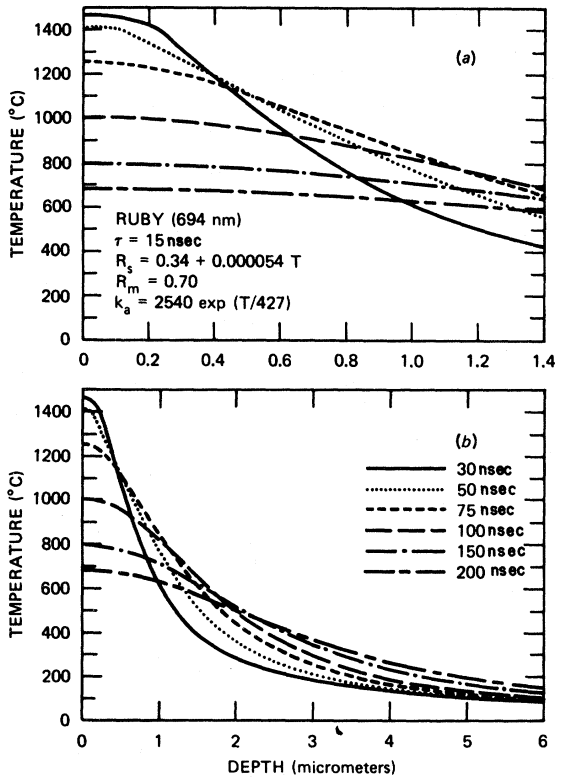

FIG. 4. Profiles of temperature vs depth, at various times after pulsed ruby-laser irradiation of c-Si at $E_I=1.2$ J/cm^2. The profiles were generated using the thermal-melting model with the parameter values given in Table I.

this carrier density could be present to a depth of order $L \sim (Dt)^{1/2} \sim 6$ μm at $t = 100$ nsec. The weighted average temperature over this depth, at $t = 100$ nsec, is $T \sim 700$ K (Fig. 4), and the temperature gradients are not large enough to produce significant carrier-confinement effects. The temperature-dependent total free-carrier absorption cross section found by Svantesson and Nilsson[34] at $\lambda = 1062$ nm is $\sigma_t = 1.7 \times 10^{-20} T$ (K) cm^2; scaling this by a factor proportional to λ^2 we obtain σ_t (1152 nm) $= 2.0 \times 10^{-20} T$ (K) cm$^2 \simeq 1.4 \times 10^{-17}$ cm^2. Thus $\alpha_{fc} = (\sigma_n n + \sigma_p p) \simeq \sigma_t n = 70$ cm^{-1}. This results in a total absorption in the depth L of order $|\Delta I / I| = L\alpha_{fc} = 0.042$, i.e., $\sim 5\%$. This estimate is in reasonably good agreement (considering the roughness of the calculation) with the experimentally observed "extra" absorption $\lesssim 10\%$ for $t \gtrsim 100$ nsec (Fig. 1).

In contrast, the additional free-carrier absorption calculated assuming only a thermally generated "intrinsic" carrier population corresponding to the $t = 100$ nsec temperature profile of Fig. 4 is less than 0.5%. Thus, the "extra" absorption appears to be due to relatively long-lived carriers that are the remnant of those carriers generated initially by absorption of the ruby-laser pulse. The presence of these long-lived carriers is directly confirmed in these same experiments, through observation of their long-lived near-band-gap photoluminescence (see Sec. III C).

B. Reflectivity

Reflectivity measurements were made using both the 633- and 1152-nm probe lasers, under both focused- and unfocused-beam conditions (see above). The spatial averaging effect of a large ($\lesssim$1-mm diam) probe spot size results in some lengthening of observed rise and fall times for transitions to and from the HRP. However, measured rise times to the HRP using focused (<200-μm diam) probe beams were $\lesssim 2$ nsec, the rise time of our Si APD detector. On the other hand, measurements of the magnitude of the reflectivity during the HRP were found to be more precise with the unfocused probe beam. This was especially true at 1152 nm, for which the probable presence of a small, but experimentally signficant, diffuse component (see above) made absolute reflectivity determination (via post-irradiation bench calibrations) less certain with the focused-beam geometry.

The transient reflectivity signals observed were similar in shape to those reported elsewhere,[5,6] and consisted of a flat-topped maximum (duration τ_m) followed by a decaying tail (duration τ_f). However, we found that the reflectivity in the HRP at 633 nm with both focused and unfocused probe beams (1152 nm with unfocused probe beam) was 2.05 (2.1) times its initial value, corresponding to reflectivities of $71 \pm 1.5\%$ ($82 \pm 5\%$). Both values are in good agreement with values calculated from the wavelength-dependent optical properties[26] of molten Si, i.e., 72% and 78% at 633 and 1152 nm, respectively. However, experiments with the focused 1152-nm beam showed an increase of the reflectivity by a factor of only 1.6, corresponding to a value of $62 \pm 4\%$ in the HRP, assuming $R_0 = 39\%$. However, if $R_0 = 46\%$ initially under focused-beam conditions (no diffuse reflection loss; see above), then the reflectivity in the HRP is $74 \pm 5\%$, again in agreement with the value for molten Si. Some earlier experiments[5,7,8] did not demonstrate that the reflectivity rises in the HRP to the values expected for molten Si; this has been cited as evidence for the inapplicability of a thermal-melting model. The results reported here remove this objection.

Transient reflectivity signals at 1152 nm also differed from those at 633 nm in exhibiting a *drop* in reflectivity, to $\lesssim 0.7 R_0$, during the first 15 nsec of the ruby-laser pulse, followed by the sudden transition to the HRP (see Fig. 5). A similar but smaller drop below R_0 also occurred following the transi-

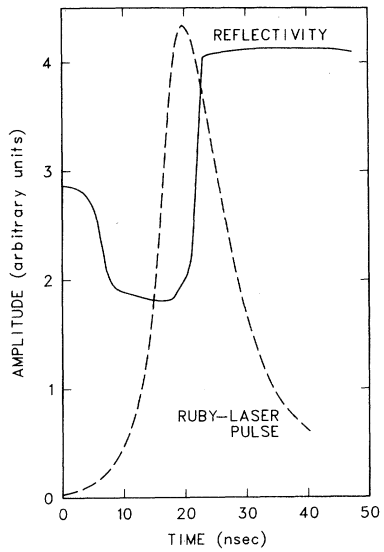

FIG. 5. Initial R drop, followed by transition to the HRP, observed with the 1152-nm probe beam. No background (baseline) corrections have been made to the vertical scale; the temporal position of the ruby-laser pulse is known within $\lesssim 5$ nsec.

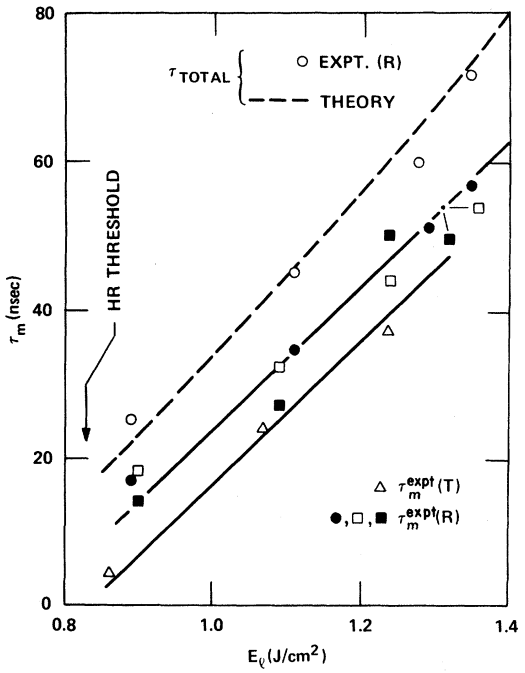

FIG. 6. E_l dependence of characteristic times in transient T and R measurements. (1) Duration of the HRP at the sample surface: - - -, theory; ○, experiment (R, using focused 633-nm probe laser). (2) τ_m, measured using focused (●) 633-nm probe beam, and focused (■) and unfocused (□) 1152-nm probe beam. (3) Duration of zero T using focused 1152-nm probe beam (△).

tion out of the HRP. The drop during the laser pulse is clear evidence for lattice heating prior to the transition to the HRP in that the increased solid-phase optical absorption (resulting from the temperature increase) eliminates multiple internal reflections; the initial reflectivity at 1152 nm then drops to the lower value ($\gtrsim 29\%$) associated with reflection at a single hot silicon-air interface.

Comparison of the duration of the HRP for a variety of probe conditions, and with the results of thermal-melting-model calculations, is made in Fig. 6. The values of τ_m measured at 1152 and 633 nm are in good agreement with each other. Furthermore, measured values of $\tau_{tot}=\tau_m+\tau_f$, where τ_f is the time required for the signal to fall to the break in the tail of the reflectivity curve (thought to represent the transition from molten to solid Si at the sample's surface[5]), are in excellent agreement with surface melt durations calculated using the thermal-melting model with the parameters given in Table I.

The threshold E_l to produce the HRP was found to be 0.86 ± 0.05 (0.80 ± 0.05) J/cm^2 using the unfocused (focused) 633-nm probe beam. Both values are in good agreement with the calculated thermal-melting threshold of 0.75 J/cm^2 for c-Si and a 15-nsec (FWHM) ruby-laser pulse.

Within the context of a thermal-melting model, τ_f is a measure of the velocity at which the recrystallizing interface approaches the sample surface.[5] Model calculations show that this velocity is expected to be a function both of the distance of the interface from the surface (slowing as it approaches the surface) and of E_l (decreasing as E_l increases).[17] We have measured the fall time corresponding to the interval between the 10% and 90% reflectivity points during the fall from the HRP. This fall time corresponds roughly to the time required for the interface to move a distance of 2.2 optical skin depths ($\sim$21.1 nm at $\lambda=633$ nm) (Ref. 26) and gives a recrystallization velocity $v=3.4\pm0.3$ m/sec for $E_l=0.9-1.1$ J/cm^2. We have also carried out a calculation of the reflectivity of a molten-Si layer, of variable thickness, on a solid hot Si substrate, which permits a more accurate estimate of the melt depths corresponding to various values of the reflectivity during the transition. This results in an average velocity between points 17.5 nm below the surface and 5 nm below the surface of 3.3 ± 0.3 m/sec for $E_l=0.9-1.1$ J/cm^2. This is in reasonable agreement with the melting-model calculation that the average velocity at a mean depth of 11 nm is 4.1 ± 0.2 (5.2 ± 0.5) m/sec for $E_l=1.2$ (1.0) J/cm^2, when it is recognized that the experiment probably underestimates v due to the effect of finite probe spot size. (It is known, from our measurements of apparent fall time versus spot size, that the recrystallizing front returns to the surface at slightly different times at different locations, thus increasing the apparent fall time and decreasing the experimental value for the velocity, as spot size increases.)

C. Photoluminescence

Experiments were also carried out without cw probe beams or bandpass filters, with the Si sample mounted directly on the Si APD enclosure, $\sim$9 mm from the detector chip. Figure 7 shows the time dependence of the intense near-band-gap photoluminescence (PL) that was detected. The radiation can be separated into two components, a sharp initial peak and a slowly decaying tail. The initial PL peak occurs $\lesssim 4$ nsec after the ruby-laser pulse peak and is comparable in width to the ruby-laser pulse. The PL peak is easily distinguished from any leakage of the ruby pulse to the detector, since the PL

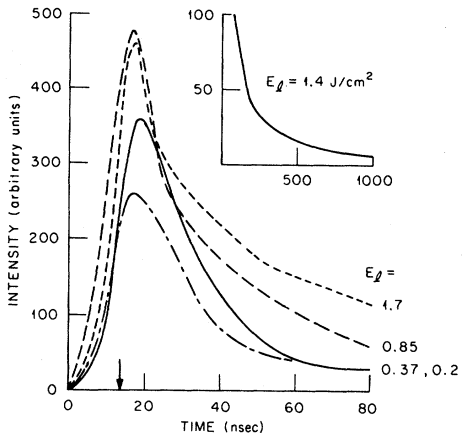

FIG. 7. Time-dependent intensity of the near-band-gap photoluminescence emitted by pulsed-laser-irradiated *c*-Si. The vertical arrow marks the position of the peak of the ruby-laser pulse. Inset: Long-time behavior of the slowly decaying tail.

peak increases less than linearly with the ruby-laser pulse intensity, and eventually saturates (Fig. 7). This initial PL peak is clearly *not* associated with the transition to the HRP, since it is prominent even at $E_l=0.2$ J/cm^2, a factor of 4 below the threshold for the HRP. The PL intensity also falls off rapidly with increasing sample-detector separation, as expected from solid angle considerations. A semilog plot of the slowly decaying PL tail reveals that several decay processes are involved, with time constants ranging from less than 100 to $\sim$1000 nsec. Similar intense recombination radiation emitted by pulsed laser-excited Si was reported by Svantesson *et al.* and by Nilsson, who ascribed the initial very rapid recombination to a third-order (Auger) band-to-band recombination process.[35] Note that the 2-mW, 1152-nm probe-laser intensity corresponds to just seven intensity units in Fig. 6, i.e., it would be completely swamped by the near-band-gap PL signal until nearly 1 μsec after the ruby-laser pulse, unless the bandpass filter is in place. We also note that no PL was detected from the silicon samples used by Compaan *et al.*[27]

IV. CONCLUSIONS

As we have shown here, thermal-melting-model calculations of the threshold for melting and of surface melt durations are in excellent agreement with measurements of the onset and duration of the high-reflectivity, zero-transmission phase in *c*-Si, using both visible and near-infrared cw probe lasers. Similarly, we have used melting-model profiles of temperature versus depth, at various times after pulsed-laser irradiation, together with new measurements of the high-temperature optical-absorption coefficient of *c*-Si at 1152 nm, to calculate the return of finite transmission after the HRP and have obtained good agreement between measured and calculated results, with no free parameters. This agreement becomes even better when the additional effect of a small amount ($\sim$5%) of free-carrier absorption is taken into account. Finally, the measured reflectivity in the HRP is in good agreement with the values expected for ordinary molten silicon at both 633 and 1152 nm. Thus, we find that there is no experimental evidence whatsoever that requires invoking the high-density plasma-annealing phase suggested by Van Vechten[24] and by Compaan.[23] The good agreement between all of our measurements and melting-model calculations also at least indirectly implies that there is probably no significant, large undercooling of molten silicon present at the recrystallizing interface, contrary to the most recent conclusion reached by Compaan,[23] since the melting-model calculations of melt-solid interface motion are carried out assuming the usual 1685-K melting point for *c*-Si. This point is further supported by an independent measurement of a recrystallization front velocity of 2.8 m/sec, using time-resolved electrical conductivity measurements following pulsed-laser irradiation of *c*-Si,[11] under conditions for which the melting model with the 1685-K melting temperature predicts a velocity of 2.7 m/sec.

ACKNOWLEDGMENTS

We would like to acknowledge helpful conversations with D. H. Auston, A. Aydinli, A. Compaan, C. L. Marquardt, S. C. Moss, and J. A. Van Vechten and assistance in sample preparation by P. H. Fleming. We also thank R. B. James for a careful review of the manuscript. This research was sponsored by the Division of Materials Sciences, U.S. Department of Energy under Contract No. W-7405-eng-26 with the Union Carbide Corporation.

[1]*Laser-Solid Interactions, and Laser Processing—1978 (Materials Research Society, Boston)* Proceedings of the Symposium on Laser-Solid Interactions and Laser Processing, edited by S. D. Ferris, H. J. Leamy, and J. M. Poate (AIP, New York, 1979).

[2]*Laser and Electron Beam Processing of Materials,* edited by C. W. White and P. S. Peercy (Academic, New York, 1980).

[3]*Laser and Electron Beam Solid Interactions and Material Processing,* edited by J. F. Gibbons, L. D. Hess, and T. W. Sigmon (North-Holland, New York, 1981).

[4]*Laser and Electron Beam Interactions with Solids,* edited by B. R. Appleton and G. K. Celler (North-Holland, New York, 1982).

[5]D. H. Auston, C. M. Surko, T. N. C. Venkatesan, R. E. Slusher, and J. A. Golovchenko, Appl. Phys. Lett. 33, 437 (1978); D. H. Auston, J. A. Golovchenko, A. L. Simons, R. E. Slusher, P. R. Smith, C. M. Surko, and T. N. C. Venkatesan, in *Laser-Solid Interactions and Laser Processing—1978 (Materials Research Society, Boston),* Ref. 1, p. 11.

[6]D. H. Lowndes and R. F. Wood, Appl. Phys. Lett. 38, 971 (1981); R. F. Wood, D. H. Lowndes, and W. H. Christie, in *Laser and Electron Beam Solid Interactions and Material Processing,* Ref. 3, p. 231.

[7]M. C. Lee, H. W. Lo, A. Aydinli, and A. Compaan, Appl. Phys. Lett. 38, 499 (1981).

[8]A. Aydinli, H. W. Lo, M. C. Lee, and A. Compaan, Phys. Rev. Lett. 46, 1640 (1981).

[9]D. H. Lowndes, Phys. Rev. Lett. 48, 267 (1982).

[10]D. H. Lowndes, G. E. Jellison, Jr., and R. F. Wood, in *Laser and Electron Beam Interactions with Solids,* Ref. 4, p. 73.

[11]G. J. Galvin, M. O. Thompson, J. W. Mayer, R. B. Hammond, N. Paulter, and P. S. Peercy, Phys. Rev. Lett. 48, 33 (1982).

[12]H. W. Lo and A. Compaan, Phys. Rev. Lett. 44, 1604 (1980).

[13]H. W. Lo and A. Compaan, Appl. Phys. Lett. 38, 179 (1981).

[14]B. C. Larson, C. W. White, T. S. Noggle, and D. Mills, Phys. Rev. Lett. 48, 337 (1982).

[15]H. P. Dumke, Phys. Lett. 78A, 477 (1980).

[16]N. Bloembergen, H. Kurz, J. M. Liu, and R. Yen, in *Laser and Electron Beam Interactions with Solids,* Ref. 4, p. 3.

[17]J. C. Wang, R. F. Wood, and P. P. Pronko, Appl. Phys. Lett. 33, 455 (1978); R. F. Wood and G. E. Giles, Phys. Rev. B 23, 2923 (1981).

[18]P. Baeri, S. V. Compisano, G. Foti, and E. Rimini, Appl. Phys. Lett. 33, 137 (1978); J. Appl. Phys. 50, 788 (1979); C. M. Surko, A. L. Simons, D. H. Auston, J. A. Golovchenko, R. E. Slusher, and T. N. C. Venkatesan, Appl. Phys. Lett. 34, 635 (1979).

[19]R. F. Wood, J. R. Kirkpatrick, and G. E. Giles, Phys. Rev. B 23, 5555 (1981).

[20]C. W. White, S. R. Wilson, B. R. Appleton, and F. W. Young, Jr., J. Appl. Phys. 51, 738 (1980).

[21]J. R. Poate, H. J. Leamy, T. T. Sheng, and G. K. Celler, Appl. Phys. Lett. 33, 918 (1978); G. J. van Gurp, G. E. Eggermont, Y. Tamminga, W. J. Stacy, and J. R. M. Gijsbers, Appl. Phys. Lett. 35, 273 (1979); J. Narayan, J. Met. 32, 15 (1980).

[22]R. F. Wood, J. C. Wang, G. E. Giles, and J. R. Kirkpatrick, in *Laser and Electron Beam Processing of Materials,* Ref. 2, p. 37; R. F. Wood, Phys. Rev. B 25, 2786 (1982).

[23]A. Compaan, A. Aydinli, M. C. Lee, and H. W. Lo, in *Laser and Electron Beam Interactions with Solids,* Ref. 4, p. 43.

[24]J. A. Van Vechten, R. Tsu, and F. Saris, Phys. Lett. 74A, 422 (1979); J. A. Van Vechten, J. Phys. 41, C4-15 (1980).

[25]S. C. Moss and C. L. Marquardt, Bull. Am. Phys. Soc. 27, 236 (1982); and in *Laser and Electron Beam Interactions with Solids,* Ref. 4, p. 79.

[26]K. M. Shvarev, B. A. Baum, and P. V. Gel'd, High Temp. 15, 548 (1977); M. O. Lampert, J. M. Koebel, and P. Siffert, J. Appl. Phys. 52, 4975 (1981).

[27]A. Compaan, private communication.

[28]H. A. Weakliem and D. Redfield, J. Appl. Phys. 50, 1491 (1979).

[29]G. E. Jellison, Jr., and F. A. Modine, Appl. Phys. Lett. 41, 180 (1982).

[30]R. F. Wood, G. E. Jellison, Jr., D. H. Lowndes, and G. E. Giles (unpublished).

[31]G. E. Jellison, Jr., and D. H. Lowndes, Appl. Phys. Lett. 41, 594 (1982).

[32]J. Dziewior and W. Schmid, Appl. Phys. Lett. 31, 346 (1977).

[33]See S. M. Sze, *Physics of Semiconductor Devices,* (Wiley-Interscience, New York, 1969), p. 38 ff.

[34]K. G. Svantesson and N. G. Nilsson, J. Phys. C 12, 3837 (1979).

[34]K. G. Svantesson, N. G. Nilsson, and L. Huldt, Solid State Commun. 9, 213 (1971); N. G. Nilsson, Phys. Scr. 8, 165 (1973).